River Flow 2010 - Dittrich, Koll, Aberle & Geisenhainer (eds) - © 2010 Bundesanstalt für Wasserbau ISBN 978-3-939230-00-7

# Measuring and modelling flow structures in a small river

Budi Gunawan, Mark Sterling, Xiaonan Tang & Donald W. Knight
*School of Civil Engineering, The University of Birmingham, Edgbaston, Birmingham, B15 2TT, UK*

ABSTRACT: As part of a project to examine the feasibility of using new measurement techniques to evaluate the conveyance capacity of a small river, acoustic Doppler current profiling (ADCP) has been deployed on a 300m stretch of the river Blackwater, Hampshire, UK. This particular reach corresponds to a doubly meandering two stage channel with various complex cross sections. Velocity data are examined for a variety of flows in order to evaluate the flow structures which exist within the channel. The work has been undertaken over a three year period which allows the impact of changes in seasonal vegetation to be examined. Finally, the applicability of using a quasi 2-D RANS model (the SKM) to model the depth averaged streamwise velocity distribution is examined.

*Keywords: Flow measurement, Floods, Numerical models, Vegetation, Velocity distribution*

## 1 INTRODUCTION

In order to accurately assess the conveyance capacity of a particular reach, it is vital to understand the resistance parameters associated with the reach. These parameters in turn affect the velocity distribution within particular cross sections and also the coherent flow patterns. These flow patterns can sometimes be observed directly and are often interpreted as flow structures or secondary flow cells. The correct representation of these flow structures in numerical models is often viewed as proof that the model is correctly calibrated. Whichever modelling approach is used (e.g. 1-D, quasi 2-D, 2-D or 3-D), detailed field measurements are important, not only for calibration, but also for yielding an insight into the true physics of the flow. With this in mind, the following paper outlines a series of experimental campaigns which were undertaken to provide detailed velocity data from several cross sections of a small meandering river. The campaigns correspond to in-bank, bankfull and over-bank flow conditions. For each campaign, information relating to the overall resistance of the reach was also evaluated.

Section 2 of the paper provides a brief overview of the test site, while section 3 outlines the instrumentation and methodology used. Section 4 outlines the data collected and interprets the flow structures by reference to the distribution of streamwise velocity and secondary flow velocity vectors. The effect of vegetation is also examined. Section 5 presents results which arise from an application of a quasi 2-D numerical model. The model simulates the depth averaged velocity distribution and illustrates that for all flow conditions, reasonable agreements can be obtained in the main channel. Finally, appropriate conclusions are drawn in section 6.

## 2 THE TEST SITE

The field measurements were conducted in a 300 m long reach of the River Blackwater, Hampshire, UK. Due to the realignment of a nearby road, a reach of the river was altered and re-engineered as a double meandering two-stage channel (Figure 1). The one-in-a-hundred year flood design capacity of the channel was 4.3 $m^3s^{-1}$, and the design bank full capacity of the main channel was 1.5 $m^3s^{-1}$. The catchment area is approximately 35 $km^2$ and the hydrological response of the reach is considered as "flashy", as the upstream reach is dominated by an urban area.

This reach has been extensively studied using a 1:5 small scale physical model (Lambert and

Sellin, 1996) and therefore an extensive database exists which enables comparisons to be made with the full-scale data. Although measurements were undertaken at several cross-sections along the reach, only the measurement results at a meandering cross-section (see Figure 1) are presented in this paper.

Approximately 100 m upstream of the inlet to the reach, shown in Figure 1, is a Sarasota electromagnetic gauging station. Hence, an independent record of the discharge at 15 minutes intervals exists. The cross section in which the Sarasota device is positioned, is approximately trapezoidal in shape. In addition, this cross section has relatively high bank elevations, which help to ensure that throughout the year, most of the flow remains in-bank (at this location only).

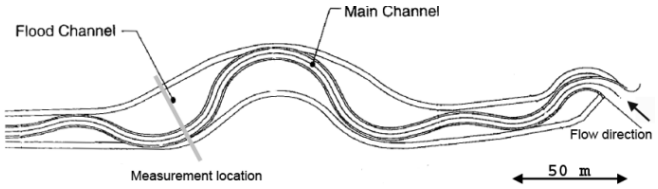


Figure 1. Plan view of the channel (after Sellin and van Beesten 2002).

## 3 INSTRUMENTATION AND METHODOLOGY

The ADCP used in the current work is the StreamPro ADCP, manufactured by Teledyne RD Instruments. The velocity data in a particular cross-section of the river is obtained by attaching the ADCP to a small boat and pulling it slowly across the river (Figure 2). Typically five to eight traverses across the river are required to enable an ensemble-average distribution to be constructed which is statistically robust. Hence, it is important to ensure that the ADCP is either located at the same position in the river, or that it traverses the same path each time. It should also be noted that if only the discharge is required, then this latter requirement can be relaxed since the discharge is frame invariant.

In order to minimise errors associated with the positioning of the ADCP, a simple winch and pulley system was devised which was fixed to the sides of the river (Figure 3). The winch and pulley system was erected at the same location during each of the measurement campaigns outlined in section 4. This simple system proved to be very effective in ensuring that the same cross section was measured during each transect (see Gunawan *et al*. 2010 for further details). In order to obtain the velocity data in a streamwise coordinate system (i.e., the main flow being normal to the cross section during in-bank flow conditions), the heading of the ADCP was required. This data was obtained by fitting a digital compass (PNI Sensor Corporation TCM 3 Tilt-Compensated Heading Module) to the boat and integrating the results with the output from the ADCP. This simple modification proved to be highly effective (Gunawan *et al.* 2010).

There are also measurement restrictions which occur when using an ADCP. For example, it is not possible to measure a narrow band near the surface as a result of the ADCP being submerged within the water. Due to technical reasons, the bottom 6% of the water depth between the transducers and the river bed should also be excluded from the measurement results. Furthermore, due to the minimum water depth requirement for undertaking measurements (0.4 – 0.5 m for the ADCP used in this research), a region at the side of each river bank cannot be measured. Notwithstanding these restrictions, the results presented below are considered sufficiently accurate for the current purposes of this research.

Six gauge boards were installed along the length of the reach in order to provide data relating to the local flow depth, from which the water surface slope could be evaluated. The results of this, for the events considered below are illustrated in Figure 4. In Figure 4, the horizontal axis represents the distance from the start of the reach and enables the location of the gauge boards to be evaluated (the data at a chainage of ~398 m corresponds the cross section under consideration). The vertical axis represents the level of the water surface above ordnance datum (AOD) or mean sea level. The dotted lines in Figure 4 represent a water surface slope ($S_W$) of $10^{-3}$. The different sets of data in Figure 4 represent the measurements made during each of the campaigns examined below, except for the December 2007 data, which were not available (see below). Finally, Figure 4 indicates that over a large section of the reach 100 m < chainage < 500 m, the water surface slope is reasonably consistent.

Figure 2. The ADCP being deployed during a flood event.

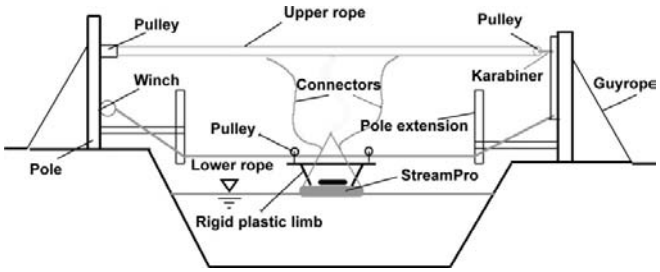


Figure 3. The winch and pulley system used in the research.

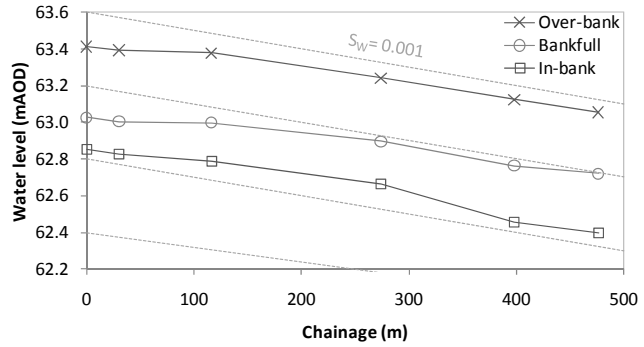


Figure 4. Water level elevations at six measurement stations during five fieldwork campaigns.

## 4 FIELD MEASUREMENT RESULTS AND ANALYSIS

### 4.1 *Experimental campaigns*

As outlined above, between five to eight transverse measurements were undertaken during each measurement campaign. The exact number depended on the variation in measured discharge between each individual run (see Gunawan (2010) for further details). Analysis of the data obtained from the Sarasota gauge indicated that during each field campaign it is reasonable to treat the discharge as steady. Furthermore, changes in the water depth during this period were always less than 1 cm, i.e., within the accuracy of the gauge boards, thus giving strength to the assumption of steady flow conditions. During the measurements, observation of the stage at the cross section was made at regular intervals (typically every 30 minutes).

The experimental campaigns were undertaken in December 2007, January 2008, August 2008 and February 2009 and correspond to in-bank flow, in-bank flow, bank-full flow and over-bank flow respectively. The timing of the two in-bank flows (i.e. one in the summer and one in winter) enabled the effect of local vegetation to be examined. The vegetation growth can be dramatic, as illustrated in Figure 5. The main hydraulic parameters corresponding to each of these events are shown in Table 1.

Table 1. Hydraulic conditions during measurements.

| | 8/2008 In-bank | 12/2007 In-bank | 01/2008 Bankfull | 02/2009 Over-bank |
|---|---|---|---|---|
| $Q$ ($m^3s^{-1}$) | 0.40 | 0.77 | 1.87 | 3.57 |
| $Re$ ($x10^5$) | 0.79 | 1.29 | 2.38 | 3.11 |
| $H$ (m) | 0.57 | 0.53 | 0.65 | 0.97 |
| $Fr$ (-) | 0.07 | 0.16 | 0.14 | 0.19 |
| $S_W$ (-) | $10^{-3}$ | N/A | $5 \times 10^{-4}$ | $7 \times 10^{-4}$ |
| $\overline{U}$ ($ms^{-1}$) | 0.17 | 0.36 | 0.61 | 0.61 |


Figure 5. Vegetation in the reach in December 2007 and August 2008.

### 4.2 *Flow structures*

Figure 6 shows the normalised streamwise velocity ($U/\overline{U}$) contours for in-bank, bank-full and over-bank flows. In Figure 6, $U$ is the local ensemble averaged streamwise velocity and $\overline{U}$ is the discharge divided by the cross sectional area. The bed profile at the measured cross-section was surveyed using a total station in 2007 and 2009 in order to monitor and record any potential changes which may have occurred. Figure 6 indicates that during the time between the two sets of survey measurements, there appears to have been some movement in the actual cross sections, with the banks moving by approximately 0.4 m in some cases. Based on photographic evidence, Gunawan (2010) suggests that this may been caused by erosion and deposition which could have taken

place during the high flow conditions which occurred between 6/12/2007 and 16/1/2008. It is, therefore, envisaged that the bed profile of the January 2008, August 2008 and February 2009 campaigns correspond to the bed profile of the 2009 survey. Most of the bed profiles measured using the ADCP (also shown in Figure 6) agree well with the bed profile measured using the total station measurements of 2009. A visible difference between the bed profiles elevations measured using both methods can be seen near the river bank in Figure 6d. This occurs as a result of the ADCP measurements being averaged from four transducers which point in four different directions. Due to this averaging, the steep bank of the cross-section is shown as a gradual change of bed elevation.

Figure 6 illustrates that there is a wide lateral variation in streamwise velocity for a given event. Furthermore, as the flow depth increases, the region of high streamwise velocity can be seen to migrate towards the inner bank of the meander (i.e., the right floodplain). In addition, the magnitude of the maximum velocity in the river increases with rising water depth.

The effect of local vegetation can also be observed by comparing Figures 6a and 6b. The vegetation effectively concentrates the majority of the flow into small regions within the channel, causing high lateral gradients of streamwise velocity.

Figure 7 illustrates the velocity vectors corresponding to the secondary flow, i.e., the flow in a plane perpendicular to the streamwise direction. As illustrated in Figures 7a – 7e a number of secondary flow cells can be observed.

In general, the lateral flow for the in-bank flow case appears to be dominated by a movement towards the outer meander (Figure 7a). This is perhaps attributable to the centrifugal force which arises as a result of the geometry of the channel at this location. However, a possible clockwise secondary cell is detected between 1.6 m < y (chainage) < 2 m. This pattern is also observed in Figure 7b. A possible anti-clockwise circulation appears at y ~ 3 m which may extend all the way to the right bank. Similar circulation patterns, but with higher strengths, appears to exist for the bank-full condition (Figure 7c).

The interpretation of secondary flow cells is to a large extent subjective, and as such it is acknowledged that an alternative interpretation could be made, i.e., four smaller cells exist between y = 1.8 m – 5.8 m.

The strength of the secondary flow corresponding to over-bank flow conditions is significantly larger than for either the in-bank or bank-full flow conditions. The anti-clockwise circulation on the right hand side still exists in the over-bank condition (Figure 7d). However, an additional anti-clockwise cell, at y = 1.6 m – 3 m, is apparent. The existence of two cells rotating in the same direction may be an artefact of the presentation of the data and could simply correspond to one large cell driven by the centrifugal force. The magnitude of the lateral velocity appears to be directly related to the magnitude of the streamwise velocity, e.g., the location of the strong lateral flow towards the outer bank near the right bank coincides with the location of the maximum streamwise velocity core.

Additional measurements were also undertaken using a Nortek 10 MHz Velocimeter (ADV) as illustrated as illustrated in Figure 7e (see Sun *et al.* (2010) for further details). Although these measurements correspond to a different measurement campaign, they confirm the above observations for the in-bank and bank-full flow conditions.

The use of the ADV enabled velocity measurements to be made on the floodplain during over-bank flow, as illustrated in Figure 7f (the main channel measurements shown in Figure 7f correspond to those presented in Figure 7d, but using a different filtering resolution). From Figure 7f it is evident that approximately half of the water on the floodplain flows towards the main channel, while the other half travels in the opposite direction.

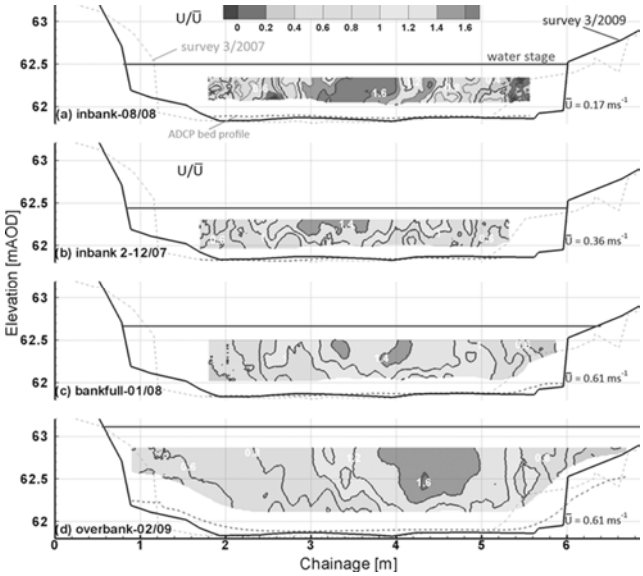

Figure 6. Normalised streamwise velocity contours.

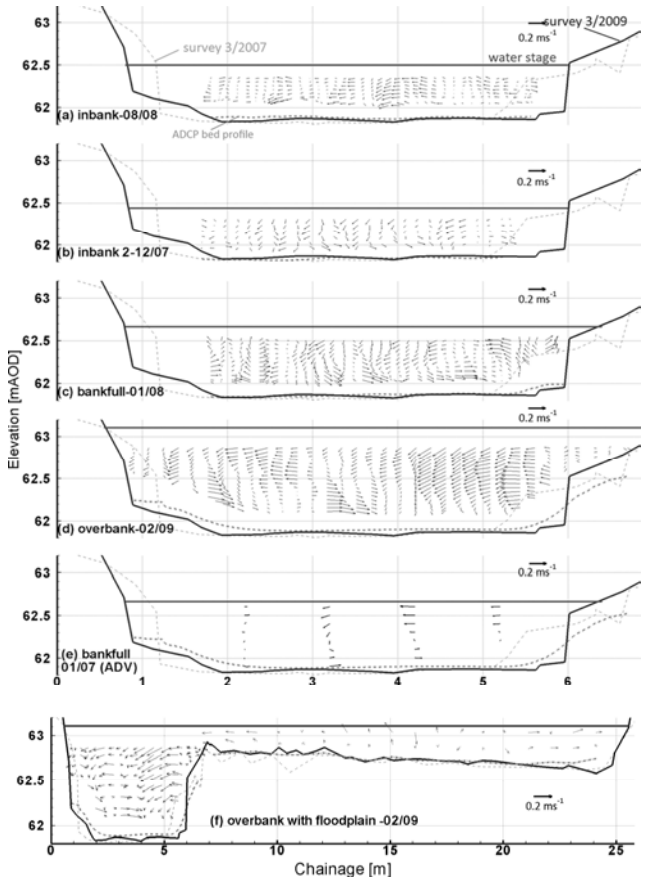

Figure 7. Velocity vectors in the lateral and vertical directions.

## 5 QUASI- 2-D NUMERICAL MODELLING OF THE RIVER BLACKWATER

As outlined in section 1, the measurements detailed in section 4 are a useful aid not only in understanding the physics of the flow but also in interpreting this behaviour in a systematic framework, i.e., a numerical model. In this respect, the Shiono and Knight method (SKM), which is fully described in several other places, (e.g., Shiono & Knight (1991), Knight & Shiono (1996) and Mc Gahey *et al*. (2010)), will be used. However, for the basis of completeness the SKM is briefly outlined below.

The governing equation for the depth-averaged velocity in a prismatic channel is assumed to be given by equation (1):

$$\rho\left[\frac{\partial(HU_d^2)}{\partial x}+\frac{\partial H(UV)_d}{\partial y}\right]=\rho g H S_o + \frac{\partial H\overline{\tau}_{xx}}{\partial x}+\frac{\partial H\overline{\tau}_{yx}}{\partial y}-\tau_b\sqrt{1+\frac{1}{s^2}} \quad (1)$$

where the overbar or the subscript *d* refers to a depth-averaged value, {*U, V*} are the velocity components in the {*x, y*} directions, with *x* = the streamwise direction parallel to the channel bed and *y* = the lateral direction, *H* = depth of flow, $\rho$ = fluid density, *g* = acceleration due to gravity, $S_o$ = bed slope of the channel, $\{\tau_{yx}, \tau_{xx}\}$ = Reynolds stresses on planes perpendicular to the *y* and x directions respectively, $\tau_b$ = boundary shear stress and *s* is the channel side slope (1:*s*, vertical: horizontal).

For flow over a flat bed, the analytical solution for $U_d$ from equation (1) is:

$$U_d=\left[A_1e^{\gamma y}+A_2e^{-\gamma y}+k\right]^{1/2} \quad (2)$$

where $A_1$ and $A_2$ are unknown constants which are obtained by applying appropriate boundary conditions, and the constants $\gamma$ and *k* are given by

$$\gamma=\sqrt{\frac{2}{\lambda}}\left(\frac{8}{f}\right)^{1/4}\frac{1}{H}\sqrt{\frac{f}{8}} \quad (3)$$

$$k=\frac{gS_oH-\Gamma/\rho}{f/8} \quad (4)$$

For flow over a linearly sloping bed is given by

$$U_d=\left[A_3\xi^{\alpha}+A_4\xi^{-(\alpha+1)}+\omega\xi+\eta\right]^{1/2} \quad (5)$$

where the constants $\alpha$, $\omega$ and $\eta$ are given by

$$\alpha=-\frac{1}{2}+\frac{1}{2}\sqrt{1+\frac{s\sqrt{1+s^2}}{\lambda}\sqrt{8f}} \quad (6)$$

$$\omega=\frac{gS_0}{\frac{\sqrt{1+s^2}}{s}\left(\frac{f}{8}\right)-\frac{\lambda}{s^2}\sqrt{f/8}} \quad (7)$$

$$\eta=\frac{-\Gamma}{\rho\sqrt{1+\frac{1}{s^2}}\left(\frac{f}{8}\right)} \quad (8)$$

In equation (5), $A_3$ and $A_4$ are unknown constants which are obtained by applying appropriate boundary conditions. (See Knight *et al*. (2004 & 2007) for further details). *f*, $\lambda$ and $\Gamma$ in equations (3) & (4) and (6) – (8) are the Darcy-Weisbach friction factor, the dimensionless eddy viscosity and the secondary flow term respectively.

In order to apply either equations (2) or (5), the cross section of the channel is subdivided into a number of panels. To a large extent, choosing the appropriate number and position of the panels is the key to obtaining an effective solution, and these choices are often informed by knowledge of the secondary flow cells, i.e., the number and location – see Knight *et al.* (2007). For the purposes of the current work, twelve panels were chosen – nine in the main channel and three on the floodplain. It was felt that this represented a reasonable trade-off between model complexity (which would arise as a result of increasing the number of

panels) and the 2-D nature of the model (i.e., the assumptions embodied within the derivation of the SKM). The distribution of the panel structure is shown in Figure 8 by the alternating series of full and dotted lines drawn on the channel bed.

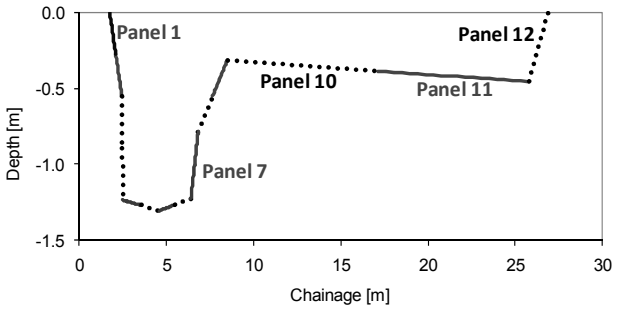


Figure 8. Panel structure for the whole cross section (c.f. Figure 9c).

The calibration of the SKM was undertaken by adjusting the values of three coefficients, namely $f$, $\lambda$ and $\Gamma$. Tang and Knight (2009) reported that for wide channels with overbank flow, the variation of $\lambda$ has a minor effect on the simulations. Hence, in order to simplify the work, a constant $\lambda$ value of 0.07 was adopted for all panels. It is recognized that this is a lower limiting value, and that values as high as 0.5 can be encountered. Initially, the parameter $f$ was calibrated for each panel while $\Gamma$ was set to zero. The comparison between simulated $U_d$ and measurements corresponding to this calibration approach is shown in Figure 9. It should be noted that the in-bank flow corresponding to December 2007 was not simulated, due to unavailability of water slope data. In what follows, it is assumed that the water surface slope ($S_w$) is approximately equal to the bed slope ($S_o$), an assumption which is supported by Figure 4.

The values of $f$ used in the simulation are shown in Table 2. High $f$ values are required in some panels, especially those corresponding to the in-bank case. Such high values are required to represent the resistance due to vegetation in the main channel (see Figure 5b) and the effect of the channel geometry, i.e., the meander. An additional momentum sink term in the RANS equation may be used to account for the effect of vegetation, rather than including it into the friction factor (e.g., see Rameshwaran and Shiono, 2007; Tang and Knight, 2009).

Figure 9a indicates the lateral distribution of depth averaged streamwise velocity for the in-bank case, August 2008. As illustrated in Figure 6a, the local velocity attains a maximum value in the centre of the channel. The results from the SKM simulation are shown by the full line and indicate that the trend is represented reasonably well. Similarly, good agreement between the simulation and measurements are also obtained for the bankfull and over-bank cases (Figures 9b and c). This good agreement is also quantified in terms of the root mean square error (RMSE), which indicates values of 0.03-0.04 $ms^{-1}$ for all cases.

Table 2. The values of parameter $f$ for each panel.

| Panel no. | In-bank | Bankfull | Over-bank |
|---|---|---|---|
| 1 | N/A | 2 | 1 |
| 2 | 10 | 2 | 1 |
| 3 | 10 | 0.25 | 1 |
| 4 | 5 | 0.15 | 0.5 |
| 5 | 0.7 | 0.08 | 0.2 |
| 6 | 1.5 | 0.09 | 0.05 |
| 7 | 3.5 | 0.09 | 0.1 |
| 8 | 3.5 | 0.2 | 0.1 |
| 9 | N/A | 0.5 | 0.8 |
| 10 | N/A | N/A | 0.8 |
| 11 | N/A | N/A | 0.8 |
| 12 | N/A | N/A | 0.8 |

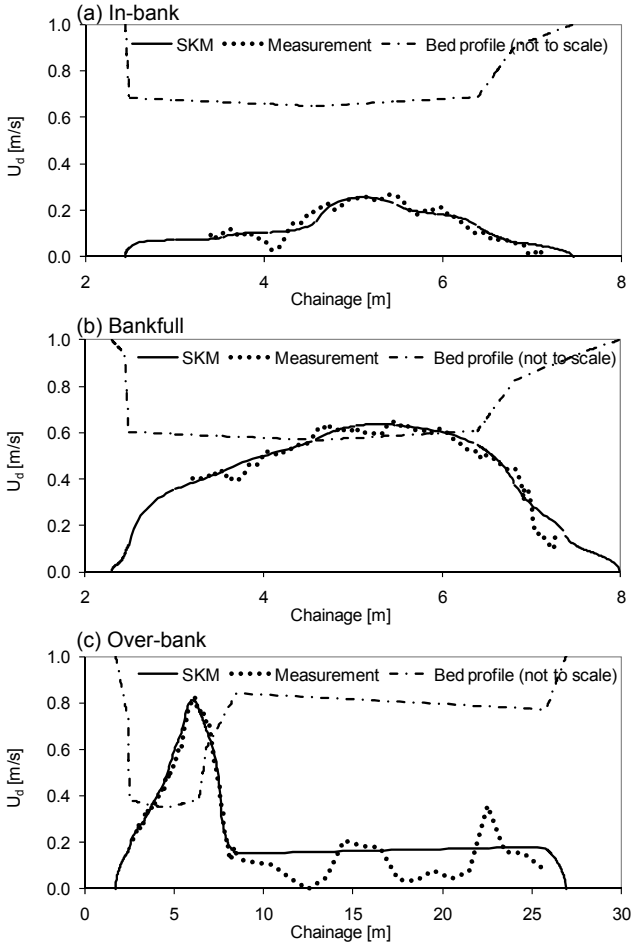


Figure 9. Comparison of simulated $U_d$ and measurement.

In order to take into account the effects of secondary flow on the numerical model, the simulation was re-calibrated using $\Gamma$ values of other than zero. This was done by altering the $f$ values in each panel to 50%, 75%, 125% and 150% of the initial $f$ values. The values of $\Gamma$ were then calibrated to obtain good agreement between simula-

tion and measurement. The $\lambda$ values for each panel were kept constant at 0.07. It can be shown that when appropriate $\Gamma$ values are chosen, the simulation results ($U_d$) for the cases with adjusted $f$ values are almost identical to that for the cases with initial $f$ values (Gunawan, 2010). It was also found that the appropriate $\Gamma$ values for each $f$ case (50%, 75%, 125% and 150% of the initial $f$ values) can be predicted using a simple linear relationship between $f$ and $\Gamma$, e.g., the relationship between $f$ and $\Gamma$ for the overbank case simulations, as shown in Figure 10. It has been demonstrated that various combination of $f$ and $\Gamma$ could yield similar results. It is, however, difficult to know which set of parameters represents the physics best, especially since the lateral distribution of $\Gamma$ values is still largely unknown. For a more in-depth discussion on this topic the reader is referred to Sharifi *et al.* (2009).

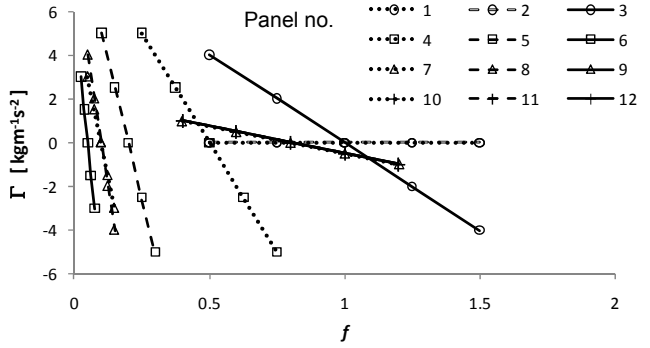


Figure 10. Calibration parameters ($f$ and $\Gamma$) used for the overbank case simulations.

## 6 CONCLUSIONS

The streamwise velocity measurements and secondary flow vectors corresponding to a variety of flow conditions, as obtained from an ADCP, have been examined. These results have tentatively been used to calibrate a quasi 2-D numerical model. The following conclusions can be made:

- there is a wide lateral variation in streamwise velocity for a given event,
- as the flow depth increases, the region of high streamwise velocity can be seen to migrate towards the inner bank of the meander,
- the magnitude of the maximum velocity in the river increases with rising water depth,
- local vegetation effectively concentrates the majority of the flow into small regions within the channel, causing high lateral gradients of streamwise velocity;
- the number of (and location of) secondary flow cells for each event is highly subjective,
- a relatively simple, quasi 2-D model can be used to simulate the events with a reasonable degree of accuracy,
- while the calibration of the quasi 2-D model is straightforward, the calibration parameters can take a wide variety of values. A physical interpretation of these values (in terms of the physics of the flow) is at the moment not available.

## ACKNOWLEDGEMENT

The authors would like to express their gratitude to the Engineering and Physical Sciences Research Council (EPSRC) for their financial support under EPSRC grant EP/E002250/1 through which this work was undertaken.

## REFERENCES

Gunawan, B., Sterling, M and Knight, D.W. 2010. Using an Acoustic Doppler Current Profiler in a small river, *Water and Environmental Journal*, CIWEM. In Press. DOI: 10.1111/j.1747-6593.2009.00170.x

Gunawan, B. 2010. A study of flow structures in a two-stage channel using field data, physical model and numerical modelling, *PhD thesis*, University of Birmingham, UK.

Knight, D.W. and Shiono, K. 1996. River channel and floodplain hydraulics, in *Floodplain Processes*, (Eds Anderson, Walling & Bates), Chapter 5, J Wiley, 139-181.

Knight, D.W., Omran, M. and Abril, J.B. 2004. Boundary conditions between panels in depth-averaged flow models revisited, *Proceedings of the 2nd International Conference on Fluvial Hydraulics: River Flow 2004*, Naples, 24-26 June, Vol. 1, 371-380.

Knight, D.W., Omran, M. and Tang, X. 2007. Modelling depth-averaged velocity and boundary shear in trapezoidal channels with secondary flows, *Journal of Hydraulic Engineering*, February, ASCE, Vol. 133, No. 1, January, 39-47.

Lambert, M.F. & Sellin, R.H.J. 1996. Velocity distribution in a large-scale model of a doubly meandering compound channel, *Wat., Marit. & Energy*, Proc. Instn Civ. Engrs, , 118.

Mc Gahey, C., Samuels, P.G. and Knight, D.W. 2010. Practical toolset for estimating channel roughness, *Water Management*, Proc. Instn of Civil Engineers, London, In Press.

Rameshwaran, P and Shiono, K. 2007. Quasi two-dimensional model for straight overbank flows through emergent vegetation on floodplains, *Journal of Hydraulic Research*, IAHR, Vol. 45, No. 3, 302-315.

Sellin, R.H.J. and van Beesten, D.P. 2002. Berm vegetation and its effect on flow resistance in a two-stage river channel: an analysis of field data. *Proc. The Interna-*

*tional Conference on Fluvial Hydraulics*, Belgium, 319 - 326.

Sun, X., Shiono,K., Chandler, J. H., Rameshwaran, P., Sellin, R. H and Fujita. 2010. Note on discharge estimation in River Blackwater using LSPIV, *Water Management*, Proceedings of the ICE –. *In Press*.

Sharifi, S., Sterling, M., and Knight, D. W. (2009) A Novel Application of a Multi-Objective Evolutionary Algorithm Applied to Open Channel Flow Modelling. Journal of Hydroinformatics. Vol. 11, No. 1, 31-50

Shiono, K. and Knight, D.W. 1991. Turbulent open channel flows with variable depth across the channel, *Journal of Fluid Mechanics*, Vol. 222, 617-646 (and Vol. 231, October, p 693).

Tang, X. and Knight, D.W. 2009. Lateral distributions of streamwise velocity in compound channels with partially vegetated floodplains. *Science In China* Series E, Technological Sciences, 52(11): 3357-3362.